

The distance to the Vela pulsar gauged with HST parallax observations.¹

P.A. Caraveo

IFC-CNR, Via Bassini 15, I-20133 Milan

pat@ifctr.mi.cnr.it

A. De Luca

IFC-CNR, Via Bassini 15, I-20133 Milan

R.P. Mignani

ESO, Karl Schwarzschild Str.2, D8574 O Garching b. München

G.F. Bignami

ASI, Via Liegi 26, I-00198 Rome

ABSTRACT

The distance to the Vela pulsar (PSR B0833–45) has been traditionally assumed to be 500 pc. Although affected by a significant uncertainty, this value stuck to both the pulsar and the SNR. In an effort to obtain a model free distance measurement, we have applied high resolution astrometry to the pulsar $V \sim 23.6$ optical counterpart. Using a set of five HST/WFPC2 observations, we have obtained the first optical measurement of the annual parallax of the Vela pulsar. The parallax turns out to be 3.4 ± 0.7 mas, implying a distance of 294_{-76}^{+50} pc, i.e. a value significantly lower than previously believed. This affects the estimate of the pulsar absolute luminosity and of its emission efficiency at various wavelengths and confirms the exceptionally high value of the N_e towards the Vela pulsar. Finally, the complete parallax data base allows for a better measurement of the Vela pulsar proper motion ($\mu_\alpha \cos(\delta) = -37.2 \pm 1.2$ mas yr $^{-1}$; $\mu_\delta = 28.2 \pm 1.3$ mas yr $^{-1}$ after correcting for the peculiar motion of the Sun) which, at the parallax distance, implies a transverse velocity of ≈ 65 km sec $^{-1}$. Moreover, the proper motion position angle appears specially well aligned with the axis of symmetry of the X-ray nebula as seen by Chandra. Such an alignment allows to assess the space velocity of the Vela pulsar to be 81 km sec $^{-1}$.

Subject headings: astrometry — stars: distances — pulsars: individual (Vela pulsar)

1. Introduction

Assessing distances to Isolated Neutron Stars (INSs) is a very challenging task which has been pursued using different techniques in different regions of the electromagnetic spectrum. Distances to pulsars with no glitching activity can be obtained through radio timing techniques (Bell 1998). However, only millisecond radio pulsars allow for positional accuracies high enough to be used for parallax measurements. Toscano et al. (1999) count 6 such cases in their list of 12 pulsars, the distances to which have been determined through parallax. For the remaining 6 objects, which are all classical pulsars with periods of few hundreds msec, a VLBI approach was used, requiring a suitable nearby calibrator. The difficulties of the VLBI technique, including the need to account for changing ionospheric conditions, are apparent from the significant revisions already published for two of the six parallax values. The parallax of PSR B0919+06 went from 0.31 ± 0.14 mas (Fomalont et al. 1999) to 0.83 ± 0.14 mas (Chatterjee et al. 2001), while for PSR B0950+08 the parallax went from 7.9 ± 0.8 mas (Gwinn et al. 1986) to 3.6 ± 0.3 mas (Brisken et al. 2000).

Even if limited to twelve objects, e.g. <1% of the pulsar family (Camilo et al. 2000), determining model-independent distances of nearby pulsars is a rewarding exercise. As summarized by Campbell et al. (1996) and Toscano et al. (1999), this allows to trace the local interstellar medium. A distance value, coupled with the pulsar dispersion measure, yields the electron density along the line of sight, to be compared with the model of the galactic N_e distribution (Taylor & Cordes 1993). Such a model is used to derive the distances to all of the remaining pulsars (>99% of the population). Moreover, a distance value transforms the pulsar proper motion into a firm transverse velocity, to be compared with the average pulsar 3-D velocities obtained by Lyne & Lorimer (1994) and Cordes & Chernoff (1998) on larger samples.

X-ray astronomy provides hints to the distance of the score of pulsars detected so far (Becker & Trümper 1997) through the measurement of the absorption of their soft X-ray emission. Unfortunately, distances derived from X-ray absorption are as uncertain as those derived by

¹Based on observations with the NASA/ESA Hubble Space Telescope, obtained at the Space Telescope Science Institute, which is operated by AURA, Inc., under NASA contract NAS 5-26555.

the dispersion measure. In general, the radio distances are greater than the X-ray ones. With the detection of pulsars in the optical (see e.g. Caraveo 2000), distance measurements became possible using classic optical astrometry techniques, based on parallax measurements. Measuring tiny parallactic displacements is never easy, and the task can become really challenging when the targets are intrinsically faint, like isolated neutron stars. It requires high angular resolution coupled with high sensitivity, rendering HST the instrument of choice to measure proper motions and parallaxes of faint objects. The astrometric capabilities of HST were used to obtain model free measurements of the distance to Geminga (Caraveo et al. 1996) and RXJ 1856–3754 (Walter 2001), two radio quiet INSs for which radio astronomy could not provide any input.

In this paper we address the Vela pulsar (PSR B0833–45) which provides a compelling case of nearby INS with a highly disputed value of the distance and a relatively bright optical counterpart ($V \sim 23.6$). The value of 500 pc, tentatively obtained after the original pulsar discovery (e.g. Milne 1968; Prentice & ter Haar 1969), has been assumed as a reference for both the pulsar and its surrounding SNR. As such, it is still quoted in radio pulsar catalogues², in spite of the doubts raised by several independent investigations carried out at different wavelengths, targeting both the pulsar and the SNR. On the basis of their analysis of the ROSAT data, Page et al. (1996) placed the Vela pulsar at 285 ± 120 pc, while Pavlov et al. (2001a), using Chandra data fitted by a two component model, obtain a distance of 210 ± 20 pc. On the other hand, studying the Vela remnant Cha et al. (1999) and Bocchino et al. (1999) find a distance of 250 ± 30 pc and ≈ 280 pc, respectively. A different view is proposed by Gvaramadze (2001) who, on the basis of the pulsar scintillation velocity and on its very uncertain interpretation, sees no reasons to revise the canonical 500 pc distance.

We started our observations aimed at the measurement of the Vela pulsar parallax in 1997, during HST observing Cycle 6, but we had to wait until Cycle 8 to complete our program. Meanwhile, our data have also been used to reassess the proper motion of the Vela pulsar (De Luca et al. 2000a) and to quantify the overall reliability of our astrometric approach (De Luca et al. 2000b). In the following we shall report the analysis of our HST data leading to the measurement of the Vela pulsar annual parallax and proper motion. The impact of our result on the current understanding of the Vela pulsar is also discussed. While HST was collecting the appropriate set of images, VLBI in the southern hemisphere came into existence and Vela was one of the targets. The preliminary radio results (Legge 2000) will be compared to our optical ones.

²see e.g. <http://www.atnf.csiro.au/Research/pulsar/psr/archive/>
or <http://pulsar.ucolick.org/cog/pulsars/catalog/>

2. The observations

The measurement of the annual parallax of a star through optical astrometry techniques requires a set of at least three observations of the field, preferably taken at the epochs of the maximum parallactic elongation. For the Vela pulsar ($\alpha_{J2000} = 08^h35^m20\rlap{.}^s.6$, $\delta_{J2000} = -45^\circ10'35\rlap{.}''.1$), the epochs of maximum parallactic elongation coincide with days 118 and 303 of the year for right ascension, and days 20 and 204 for declination, with relative parallax factors (see e.g. Murray, 1983) at the maximum elongation of ≈ 0.97 and ≈ 0.90 , respectively (see Figure 1). Although the relative parallactic factor at maximum elongation is somewhat larger in right ascension, observations at one of the corresponding epochs turned out to be difficult to schedule, due to their very tiny visibility window. For this reason, the observations of Vela were scheduled close to the epochs of the maximum parallactic displacements in declination.

Our program was originally approved for HST Cycle 6 but, unfortunately, only two observations of the planned triplet were executed. The whole program had to go through a new approval cycle and was rescheduled and successfully completed in Cycle 8. We thus obtained a total of five observations of the field with the WFPC2 between June 1997 and July 2000. The complete journal of the observations is summarized in Table 1. At each epoch, two exposures of the field were acquired with the WFPC2 “V” filter $F555W$ ($\lambda = 5252\text{\AA}$, $\Delta\lambda = 1225\text{\AA}$) and with similar integration times. In order to maximize the angular resolution, in all cases the pulsar optical counterpart was centered on the Planetary Camera chip (PC) of the WFPC2 (pixel size of 0.045 arcsec).

3. Data reduction and analysis

The data reduction was performed using the IRAF/STSDAS package. After the standard pipeline processing of the frames (debiasing, dark subtraction, flatfielding), which was performed using the most recent reference files and tables, each couple of coaligned images was co-added for a first filtering from cosmic ray hits. Residual hits were later rejected using specific cosmic ray subtraction algorithms in IRAF. Figure 2 shows the resulting image for July 2000.

The cleaned images have then been used for the definition of a relative reference frame to be used as a starting point for our astrometric procedure. Since all the observations have been taken with different telescope roll angles and with small relative offsets, the definition of a relative reference frame must rely on a very accurate image superposition. Following the approach applied successfully in previous astrometric works (e.g. Caraveo et al. 1996; Caraveo and Mignani 1999; De Luca et al. 2000a; Mignani et al. 2000a, Mignani et al. 2000b), this

is done by computing a linear coordinate transformation (i.e. accounting for 2 independent translation factors, 2 scale factors and a rotation angle) between a set of reference objects. The selection of the reference grid objects is critical. They must be point-like, present in all observations (but not too close to the field edges), bright enough to allow for an accurate positioning (but not saturated). A set of 26 such objects (labeled in Figure 2) was selected in the reference frame of the PC.

Since the shape of the PC Point Spread Function (PSF) is known to be position-dependent (Krist 1995), we did not use simulated PSFs for source fitting. On the other hand, the number of good reference stars was not sufficient to compute a template PSF directly from the images. Thus, the reference object coordinates were computed by fitting a 2-D gaussian function to their intensity profiles, using optimized centering areas. This yielded positional uncertainties of the order of $0.01 \div 0.05$ pixel, depending on the objects' brightness and position on the chip. Special care was devoted to characterizing the errors involved in the centroid determination. Following De Luca et al. (2000b), we addressed both statistical errors (i.e. due to each object's S/N) and systematic ones (due, e.g., to the telescope jitter, defocussing of the camera, charge transfer in the CCD, background fluctuations, etc.). Moreover, we checked that our results were not biased by the algorithm used for the fitting. The coordinates were corrected for the “34th row error” (Anderson & King 1999) and for the significant, well-known, instrument geometrical distortion using the most recent mapping of the PC field of view (Casertano & Wiggs 2000). The centroids of the Vela pulsar optical counterpart were obtained in the same way, yielding errors ranging between 0.02 and 0.04 pixel.

Having secured a reference grid, we registered all the frames on the June 1999 one, taken as a reference and previously aligned along right ascension and declination according to the telescope roll angle. The rms of the residuals on the reference object coordinates were < 0.05 pixel in right ascension and < 0.04 pixel in declination. The overall accuracy of the frame registration, accounting for errors in the centroid determination as well as in the geometric distortions mapping, and the accuracy of the fit, has been discussed in detail by De Luca et al. (2000b).

To ensure that our procedure was not affected by any displacement of our 26 reference objects (due either to proper motions or parallaxes), we have repeated the frame registration 26 times, i.e. each time excluding one of the objects from the fit. In addition, to exclude any possible bias due to the arbitrary choice of the reference frame, we have repeated the whole procedure cycling it over the five epochs. In all cases, we obtained statistically undistinguishable results. We are thus confident that our procedure is correct and free of systematics. Last, we have applied the coordinate transformations to the positions of the Vela pulsar; the resulting relative positions are shown in Figure 3.

If fitted with a simple proper motion, all the points in Figure 3 are seen to deviate from

the straight line. Their residuals wrt the proper motion fit, however, are not randomly distributed. Rather, they follow the trend expected for an object affected also by parallactic displacement.

4. Analysis of the pulsar displacements

The geocentric right ascension and declination $(\alpha_G(t), \delta_G(t))$ of the pulsar at a given epoch t can be expressed in the form

$$\begin{cases} \alpha_G(t) = \alpha_B(t_0) + \mu_\alpha \cos(\delta)(t - t_0) + \pi P_\alpha(t) \\ \delta_G(t) = \delta_B(t_0) + \mu_\delta(t - t_0) + \pi P_\delta(t) \end{cases} \quad (1)$$

where $(\alpha_B(t_0), \delta_B(t_0))$ are the barycentric coordinates at a reference time t_0 , (μ_α, μ_δ) are the right ascension and declination components of the proper motion, π is the annual parallax and $(P_\alpha(t), P_\delta(t))$ are the parallactic factors shown in Figure 1. A system of equations like (1) can be written for each of the five epochs corresponding to our observations.

Setting $t_0=1999$, June 30 as the reference epoch, one can obtain five pairs of equations relating the observed coordinates of the pulsar to the 5 unknowns π , μ_α , μ_δ , $\alpha_B(t_0)$ and $\delta_B(t_0)$. A least squares fit yields for the parallax and the proper motion the following values: $\pi = 3.4$ mas, $\mu_\alpha \cos(\delta) = -45.0$ mas yr^{-1} , $\mu_\delta = 25.8$ mas yr^{-1} , corresponding to a reduced χ^2 of 0.11 (5 degrees of freedom).

To evaluate the uncertainties and the confidence levels on the fitted parameters, we ran a MonteCarlo simulation for a theoretical source featuring proper motion and parallax values equal to our best fit ones. Each synthetic data set was obtained by perturbing a coordinate set representing the expected source geocentric positions at the epochs of our observations. The experimental error (per coordinate) for each data point in each simulated data set was computed from a normal distribution with a standard deviation equal to the overall uncertainty (per coordinate) affecting the pulsar positioning estimated in sect. 3 (i.e. ≤ 2 mas per coordinate in 1999, June 30; $2.5 \div 2.9$ mas per coordinate in the remaining epochs). After 10^5 simulations, we estimate the 1σ error bar, to be attached to the parallax value, at 0.7 mas, while the uncertainties on the proper motion are 1.1 mas in α and 1 mas in δ . Thus, our best evaluation of the Vela pulsar displacements is as follows:

$$\begin{aligned} \pi &= 3.4 \pm 0.7 \text{ mas} \\ \mu_\alpha \cos(\delta) &= -45.0 \pm 1.1 \text{ mas } \text{yr}^{-1} \\ \mu_\delta &= 25.8 \pm 1.0 \text{ mas } \text{yr}^{-1} \end{aligned}$$

corresponding to a position angle of $299.8^\circ \pm 1.2^\circ$.

The Vela path in the sky, as predicted from the best fitting proper motion and parallax, is plotted in Figure 4, together with the measured pulsar positions. The agreement between the expected positions and the measured ones is remarkably good.

4.1. The proper motion

Our best fit to the pulsar proper motion improves the result of De Luca et al. (2000b) by confirming the overall value but by further reducing its associated errors. Since we measure the Vela proper motion with respect to a set of reference stars in the field, our value is sensitive to the peculiar motion of the Sun in the Local Standard of Rest. This induces an apparent annual displacement of the pulsar in the anti-Apex direction, which should be corrected for in order to evaluate the pulsar motion with respect to the structures located in its immediate surroundings (such as the synchrotron nebula detected in X-rays). A word of caution is required, since the correction depends critically on a reliable definition of the LSR. Following the analysis of Dehnen & Binney (1998), based on Hipparcos data, we assumed a peculiar motion of the Sun of 13.4 ± 0.8 km/s in the direction $l = 28 \pm 3^\circ$, $b = 32 \pm 2^\circ$. The components of the proper motion of the Vela pulsar with respect to the LSR become $\mu_\alpha \cos(\delta) = -37.2 \pm 1.2$ mas yr $^{-1}$, $\mu_\delta = 28.2 \pm 1.3$ mas yr $^{-1}$, for a resulting position angle of $307.2 \pm 1.6^\circ$. We note that a very similar result ($\mu_\alpha \cos(\delta) = -38.3 \pm 1.2$ mas yr $^{-1}$, $\mu_\delta = 27.4 \pm 1.3$ mas yr $^{-1}$, P.A.= $305.6 \pm 1.6^\circ$) is obtained using the correction for the Sun peculiar motion adopted by Bailes et al.(1989).

4.2. The annual parallax

The value of the pulsar annual parallax which best fits our data is 3.4 ± 0.7 mas. The probability of obtaining such a value in absence of any parallactic displacement is of the order 10^{-5} . From our parallax value we can derive the distance to the Vela pulsar, which turns out to be:

$$294_{+76}^{-50} \text{ pc}$$

We can now compare our results on the Vela proper motion and parallax with the preliminary radio ones obtained by Legge (2000), e.g., $\mu_\alpha \cos(\delta) = -49.8 \pm 0.2$ mas yr $^{-1}$, $\mu_\delta = 30.5 \pm 0.1$ mas yr $^{-1}$ and $\pi = 3.13 \pm 0.33$ mas. While his parallax value is similar to ours, his proper

motion values are not compatible with those obtained using the HST both for the study of "pure", parallax-free, proper motion (De Luca et al. 2000b) and for our parallax fit. However, no details are available on the calibrator used, nor on the ionospheric correction approach, nor on the correction for galactic rotation (on top of the Sun peculiar motion), so that we cannot assess the accuracy of the radio data analysis. Since the optical approach we have used is free from all such systematics, we conclude that our distance determination based, as it is, on direct measurement, with well known error determination procedure, is to be taken as the most reliable estimate to the true distance of this celestial object.

5. Discussions

After Geminga (Caraveo et al. 1996) and RXJ1856-3754 (Walter 2001), this is the third measurement of the optical parallax of an isolated neutron star, to be added to the list of a dozen radio parallaxes summarized by Toscano et al. (1999). At variance with the two previous cases, that had no firm distance estimates, the new value for the distance of the Vela pulsar is significantly smaller than the traditionally accepted one, confirming the earlier claims by Page et al. (1996), Bocchino et al. (1999), Cha et al. (1999) and Pavlov et al. (2001a).

While adding an important piece of information to the distribution of electrons in the local environment, a distance of ≤ 300 pc has several implications for the Vela pulsar physics, as well as for its kinematics. In what follows we shall address each of these points.

5.1. Local Interstellar Medium

Toscano et al. (1999) used the 12 radio pulsars with a measured parallax to map the local interstellar medium and deduce electron densities along their different lines of sight. The Vela pulsar was added to the sample on the basis of the distance of 250 pc, suggested by Cha et al. (1999) for the SNR. Coupling the Vela DM (67 cm^{-3}) with such a distance, Toscano et al. (1999) computed an N_e of 0.270 cm^{-3} , to be compared with the average density of 0.02 cm^{-3} of the Taylor & Cordes (1993) model for the local region. Indeed, the N_e towards Vela is the maximum in their sample and it is 5 to 10 times higher than the values found for four other pulsars in the 3rd galactic quadrant. These pulsars already show N_e values systematically higher than a comparable number of objects in the first galactic quadrant. Our distance value, while slightly lowering the N_e value to 0.23 cm^{-3} , confirms the extremely high electron density towards Vela, possibly pointing towards the existence of ionised clouds in the Vela region direction, at the edge of the so called β CMa

tunnel. This problem has been recently addressed by Cha et al. (2000) who, doing the "astronephography" of the region (3-D mapping of interstellar clouds), found three distinct absorption systems with different velocities, consistent with an enhanced density of ionized material towards PSR B0833-45.

5.2. Multiwavelength emission

For twenty years, up to 1993, the Crab and Vela pulsars were the only neutron stars detected throughout the entire electromagnetic spectrum, from radio to optical to high-energy γ -rays. Remarkably similar in high energy γ -rays, the behavior of the two pulsars is very different at all other wavelengths (see e.g. Thompson. 2001). Furthermore, our current understanding of the pulsar emission mechanisms at wavelengths other than radio has been biased by the phenomenology of Crab and Vela, since theories have been shaped to account for the multiwavelength behavior of these two objects. The significant downsizing of the Vela pulsar luminosity (by a factor of $\approx 3 \pm 1$) presented here, implies some revision on the current view of pulsars multiwavelength behavior. However, lowering the distance to the Vela pulsar does not have the same impact in the various spectral domains.

Vela has a very special place in the high energy γ -ray sky where it is by far the brightest source, outshining the Crab by a factor of ≈ 4 . Its radiation is totally pulsed (Kambach et al. 1994) and its spectral shape varies throughout the light curve. Of course, to convert the measured flux into a luminosity one needs to know the pulsar distance, together with its beaming factor. While the γ -ray community never disputed the traditional 500 pc value for the Vela distance, the beaming solid angle remains unknown, ranging from the size of a neutron star polar cap to 4π for isotropic emission (see Thompson et al. 1999 and references therein). For simplicity, a 1 sr conical beam is generally assumed, yielding a beaming factor of $1/4\pi$. With such a beaming value, the high energy luminosity of the Vela pulsar is now 7×10^{33} erg sec $^{-1}$, comparable to that of the much older PSR B1055-52 and 10 times lower than that of PSR B1706-44, a pulsar remarkably similar to Vela in its P , \dot{P} and overall energetics. Moreover, the efficiency with which Vela converts its rotational energy loss into γ -rays becomes 0.001, similar to that of the much younger Crab and 20 times smaller than that of PSR B1706-44. Not surprisingly, the Vela pulsar is now well below any best fitting line correlating the γ -ray luminosity to pulsar parameters such as the number of accelerated particles (Thompson et al. 1999) or the value of the open field line voltage (Thompson 2001). This will require a critical re-examination of the position of Vela in the γ -ray emitting pulsar family. Vela may become an underluminous pulsar, an apparent paradox considering its brightness in the γ -ray sky.

In the X-ray domain, the situation is different. The X-ray emission phenomenology already

prompted a number of authors (Page et al. 1996; Pavlov et al. 2001a; Helfand et al. 2001) to opt for a distance smaller than the “canonical” one. Indeed, for a distance of 500 pc, the soft X-ray flux, most probably originated by the hot surface of the neutron star, pointed towards an emitting area ($R^\infty = 3 \div 4$ km) far too small to be compatible with the whole neutron star surface (Ögelman et al. 1993). On the other hand, a very small emitting hot spot is obviously incompatible with the shallow pulsation seen at these energies. Reducing the pulsar distance to half its “canonical” value, Pavlov et al. (2001a) find that for a pure black-body emission, a radius of the emitting area of just $1.9 \div 2.4$ km could explain the flux observed by Chandra. Introducing a modified black body with a pure H atmosphere eases the emitting area problem, allowing for the whole surface of a 13 km radius neutron star at 210 pc to emit at a temperate significantly smaller than that obtained in the pure black body case. Our new independent distance determination now freezes one of the parameters of the model, allowing for a better determination of both the neutron star radius and its temperature.

The parallax distance fixes the overall Vela X-ray luminosity (0.2-8 keV) to be about $5.5 \cdot 10^{32}$ erg/sec, divided between a thermal component, dominating at low energies, and a non thermal one, emerging only at higher energies. If compared to the available rotational energy loss, such an X-ray emission accounts for $8 \cdot 10^{-5}$ of the pulsar reservoir, significantly less than the average ratio of $\approx 10^{-3}$ found for the majority of the young X-ray emitting pulsars (Becker & Trümper 1997). Moreover, such an already low conversion efficiency shrinks to 10^{-6} if one considers only the non-thermal component, confirming the severe underluminosity of PSR 0833-45 in the X-ray domain. The interpretation of such an underluminosity is, however, complicated by the composite nature of the Vela emission. It is certainly dominated by thermal emission for $E \leq 1.8$ keV, with a weaker magnetospheric component emerging only at $E \geq 1.8$ keV Pavlov et al. (2001a). Because of such a composite nature, the Vela pulsar X-ray emission cannot be readily compared to other purely magnetospheric cases (e.g the Crab and PSR B0540-69).

The X-ray data can also be used to further map the local ISM. The comparison between distance and Hydrogen column density, N_H , responsible of the X-ray absorption, provides an assessment of the reliability of this parameter as a distance indicator for nearby sources. In the optical domain, the reduction in the pulsar luminosity has important implications. Here the emission is certainly magnetospheric - as witnessed by its double-peaked light curve (Wallace et al. 1977; Manchester et al. 1978; Gouiffes 1998) and by its flat $3600 \div 8000$ Å spectrum (Nasuti et al. 1997; Mignani & Caraveo 2001). However, the revised value of the B-to-U optical luminosity $L_{BU} \approx 5.5 \cdot 10^{28}$ erg sec $^{-1}$ is now quite low with respect to the prediction of the classical Pacini & Salvati (1983) model, based on synchrotron emission at the light cylinder. Such an underluminosity could neither be ascribed to the spectral shape of the optical emission, which is remarkably similar to the Crab one (Mignani and Caraveo,

2001), nor to the shape of the light curve (see e.g. Gouiffes, 1998), which covers a broader phase interval than the Crab one, resulting, if anything, in an increase of the optical output. The behaviour of the Vela pulsar in the optical domain should be considered in the light of its “transition” position between the group of the young energetic pulsars, characterized by pure magnetospheric emission and the middle-aged ones characterized by composite spectra and lower emission efficiency (see e.g. Caraveo, 1998; Mignani and Caraveo, 2001).

In the X-ray domain Vela behaves as a middle-aged object (see e.g. Pavlov et al, 2001a) while in the optical and gamma-ray energy ranges its phenomenology is reminiscent of that of the younger pulsars but with a low emission efficiency. The multiwavelength luminosities of the Vela pulsar, stemming from the newly determined distance, will help to discriminate the emission mechanisms at work in the different energy domains and to assess their evolution throughout the life of the pulsars.

5.3. Proper motion

The parallax fit yields also, as a by-product, the best proper motion value obtained so far at optical wavelengths, corresponding to a transverse velocity of $\approx 65 \text{ km sec}^{-1}$. The space direction of the Vela proper motion has been correlated with the axis of symmetry of the Chandra X-ray structure by a number of authors (Mignani et al. 2000b, Helfand et al. 2001 and Pavlov et al. 2001b). Since the X-ray nebula axis of symmetry should trace the pulsar rotational axis, an alignment between such axis of symmetry and the pulsar proper motion would have important bearings of the kick mechanism responsible for the neutron star ejection. Lai et al. (2001), noting that proper motion-axis of symmetry alignment seems to be present also for the Crab pulsar (Caraveo & Mignani 1999), considered different spin-kick alignment mechanisms. Also in view of the pulsars’ low velocities, they concluded that both natal kicks, be they hydrodynamic or neutrino-magnetic, as well as postnatal ones, such as the Harrison and Tademaru (1975) electromagnetic kick, could account for the alignments.

Here, we reassess the case for the Vela proper motion X-ray jet alignment by comparing our “corrected” proper motion position angle (p.a.) of $307.2^\circ \pm 1.6^\circ$ with the value of $307^\circ \pm 2^\circ$ computed by Pavlov et al. (2001b) for the axis of symmetry of the structure seen by Chandra. Assuming an uniform probability distribution for the two vectors in space, we estimate the chance occurrence probability to be $1.2 \cdot 10^{-3}$, thus strengthening the case for an alignment between the Vela rotation axis and its proper motion. Figure 5 shows an update of Figure 2 of Mignani et al. (2000b), with our corrected proper motion vector superimposed to the high resolution Chandra image of the Vela nebula. Taking advantage of such an alignment we can use the angle of 53.2° , computed by Helfand et al (2001) between the axis

of the X-ray torus and the line of sight, to convert our measured transverse velocity into the pulsar 3-D velocity. Thus, the space velocity of the Vela pulsar turns out to be 81 km/sec. While hardly compatible with the Lyne & Lorimer (1994) mean value of 400 km sec⁻¹, our value is also in the low side of the low velocity component of the bimodal fit by Cordes & Chernoff (1998), classifying Vela as a rather slow moving pulsar.

6. Conclusions

We have presented the first direct measurement of the distance to the Vela pulsar at optical wavelengths. Our value is significantly smaller than the canonical one, implying a downgrading of the luminosity of the Vela pulsar, positioning Vela among the underluminous pulsars. High energy γ -ray astronomy is the most affected by our result since it pertains to the brightest, hence most conspicuous, source in the γ -ray sky. The optical domain is also seriously affected by our overall luminosity reduction, while the X-ray side is only marginally altered. The distance determination also confirms the anomalously high density of electrons towards the Vela pulsar, pointing to the presence of ionized clouds in the local interstellar medium.

As a byproduct of the parallax fit, we have obtained a very accurate proper motion value, which appears nicely aligned along the axis of symmetry of the X-ray nebula, hence the pulsar rotation axis. Moreover, our proper motion, together with our distance determination, fixes the transverse velocity of Vela to 65 km sec⁻¹. Using the inclination of the X-ray torus, as measured by Helfand et al (2001), we can convert our transverse velocity into the 3-D one, yielding a value of 81 km sec⁻¹. For a pulsar, this is certainly a low velocity.

7. Acknowledgements

This work was supported by the Italian Space Agency (ASI). We thank the referee, David Chernoff, for his suggestions.

REFERENCES

Anderson, J. & King, I.R. 1999, PASP, 111, 1095
Bailes, M., Reynolds, J.B. & Manchester, R.N. 1989, ApJ, 343, L53

Becker, W. & Trümper, J. 1997, A&A, 326, 682

Bell, J.F. 1998, AdSpR, 21, 137

Bocchino, F., Maggio, A., & Sciortino, S. 1999, A&A, 342, 839

Brisken, W.F. et al. 2000, ApJ, 541, 959

Camilo, F. et al. 2000, in ASP Conf.Ser. 202, Pulsar Astronomy - 2000 and Beyond, ed. M. Kramer, N. Wex, and N. Wielebinski, (San Francisco: ASP), p.3

Campbell, R.M. et al. 1996, ApJ, 461, L95

Caraveo, P.A., Bignami, G.F., Mignani, R. & Taff, L.G. 1996, ApJ, 461, L91

Caraveo, P.A. 1998, Advances in Space Reserch, 21,187

Caraveo, P.A. & Mignani, R.P. 1999, A&A, 344, 367

Caraveo, P.A. 2000, in ASP Conf.Ser. 202, Pulsar Astronomy - 2000 and Beyond, ed. M. Kramer, N. Wex, and N. Wielebinski, (San Francisco: ASP), p.289.

Casertano, S. & Wiggs, M.S. 2000, see WFPC2 Instrument Handbook v5.0, 2000, ed. STScI

Cha, A.N., Sembach, K.R. & Danks, A.C. 1999, ApJ, 515, L25

Cha, A.N., Sahu, M.S., Moos, H. & Blaauw, A. 2000, ApJS, 129, 281

Chatterjee, S., Cordes, J. M., Lazio, T. J. W., Goss, W. M., Fomalont, E. B. & Benson, J. M. 2001, ApJ, 550, 287

Cordes, J.M. & Chernoff, D.F. 1998, ApJ, 505, 315

Dehnen, W. & Binney, J.J. 1998, MNRAS, 298, 387

De Luca, A., Mignani, R.P. & Caraveo, P.A. 2000a, A&A, 354, 1011

De Luca, A., Mignani, R.P. & Caraveo, P.A. 2000b, to appear in the proc. of the Symp. A Decade of HST Science, Baltimore, April 11 - 14, 2000, astro-ph/0009034

Fomalont, E. B., Goss, W. M., Beasley, A. J. & Chatterjee, S. 1999, AJ, 117, 3025

Gouiffes, C. 1998, Proc. Neutron Stars and Pulsars: 30 years after the discovery, Eds. N.Shibasaki, N.Kawai, S. Shibata & T. Kifune, p.363, Universal Academic Press

Gvaramadze, V. 2001, A&A, 369, 174

Gwinn, C. R., Taylor, J. H., Weisberg, J. M. & Rawley, L. A. 1986, AJ, 91, 338

Harrison, E.R., & Tademaru E. 1957, ApJ 201, 447

Halford, D.J., Gotthelf, E.V. & Halpern, J.P. 2001, ApJ, in press, astro-ph/0007310

Kambach, G. et al. 1994, A&A, 289, 855

Krist, J. E. 1995, in Calibrating Hubble Space Telescope: Post Servicing Mission, eds. A. Koratkar and C. Leitherer, p. 311.

Lai, D., Chernoff, D. F. & Cordes, J. M. 2001, ApJ, 549, 111

Legge D. 2000, in ASP Conf.Ser. 202, Pulsar Astronomy - 2000 and Beyond, ASP Conference Series, Vol. 202, p. 141, ed. M. Kramer, N. Wex, and N. Wielebinski

Lyne, A.G. & Lorimer, D.R. 1994, Nature, 369, 127

Manchester, R.N., et al. 1978, MNRAS, 184, 159

Mignani, R.P., De Luca, A. & Caraveo, P.A. 2000a, ApJ, 543, 318

Mignani, R.P., Caraveo, P.A. & De Luca, A. 2000b, to appear in the proc. of the Symp. A Decade of HST Science, Baltimore, astro-ph/0009033

Mignani, R.P. & Caraveo, P.A. 2001, A&A, in press astro-ph/0107027

Milne, D.K. 1968, Australian J. Phys., 21, 201

Murray, A.C. 1983, "Vectorial Astrometry", Adam Hilger Ltd., Bristol

Nasuti F.P., Mignani R.P., Caraveo P.A. & Bignami G.F. 1997, A&A, 323, 839

Ögelman, H., Finley, J.P. & Zimmerman, H.U. 1993, Nature, 361, 136

Pacini, F. & Salvati, M. 1983, ApJ, 274, 369

Page D., Shibanov Y.A. & Zavlin V.E. 1996, in proc. 'Roentgenstrahlung from the Universe', ed. H.U. Zimmermann, J.Trumper, H.Yorke, MPE Report 263, p. 173

Pavlov, G.G., Zavlin, V.E., Sanwal, D., Burwitz, V. & Garmire, G. 2001b, ApJ, 552, L129

Pavlov, G.G., Kargaltsev, O.Y., Sanwal, D. & Garmire, G.P. 2001b, ApJ, 554, L189

Prentice, A.J.R. & Ter Haar, D. 1969, MNRAS, 146, 423

Spruit, H. & Phinney, B.S. 1998, *Nature*, 393, 139

Taylor, J.H. & Cordes, J.M. 1993, *ApJ*, 411, 674

Toscano, M. et al. 1999, *ApJ*, 523, L171

Thompson, D. J et al. 1999, *ApJ*, 516, 297

Thompson, D.J. 2001, to appear in the proceedings of the International Symposium on High-Energy Gamma-Ray Astronomy, 2000, Heidelberg, astro-ph/0101039

Wallace, P.T. et al. 1977, *Nature*, 266, 692

Walter, F.M. 2001, *ApJ*, 549, 433

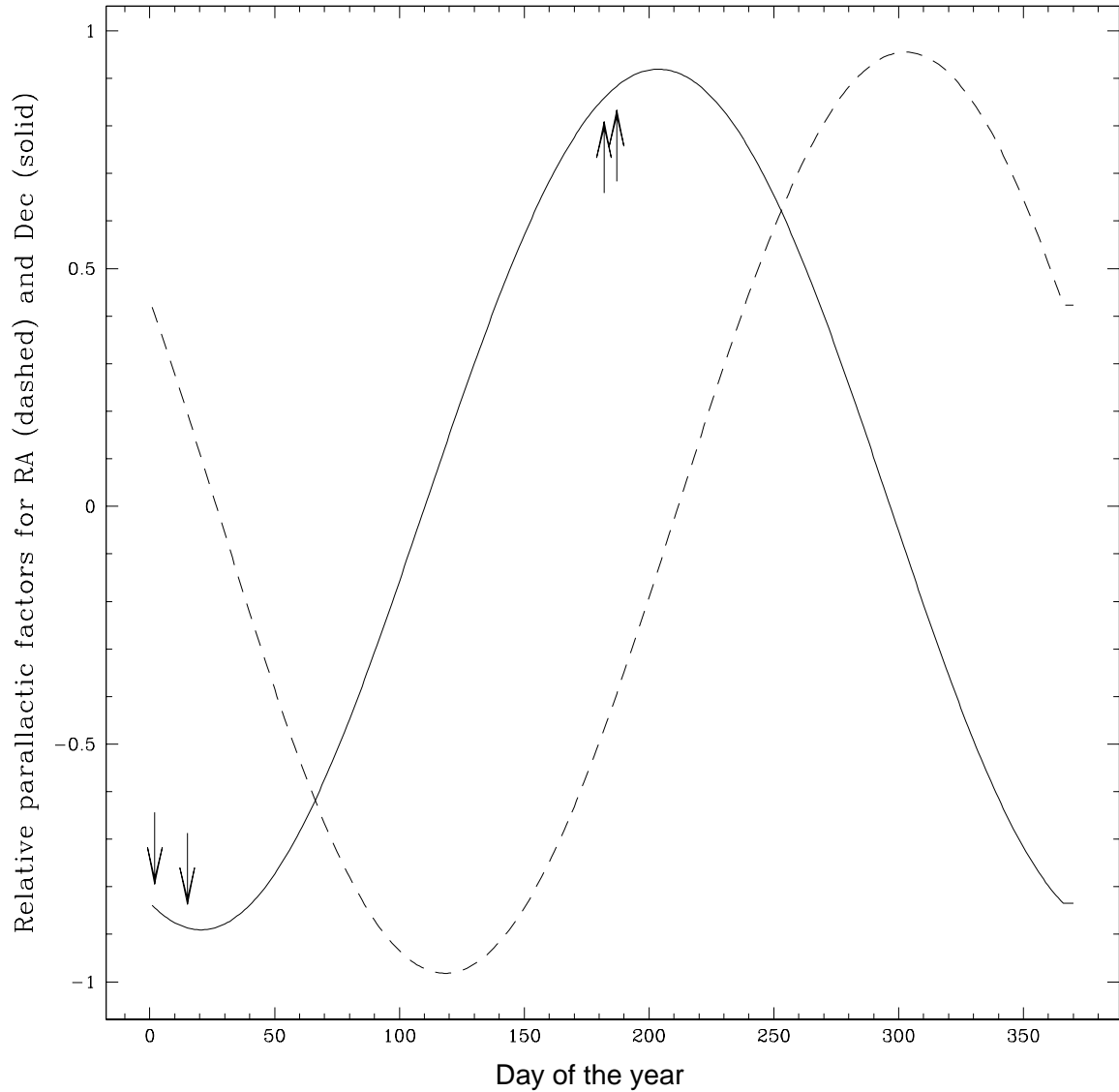


Fig. 1.— Relative parallactic factors in right ascension (dashed) and declination (continuous) computed for the Vela pulsar position. The arrows mark the periods of the year corresponding to the observations listed in Table 1.

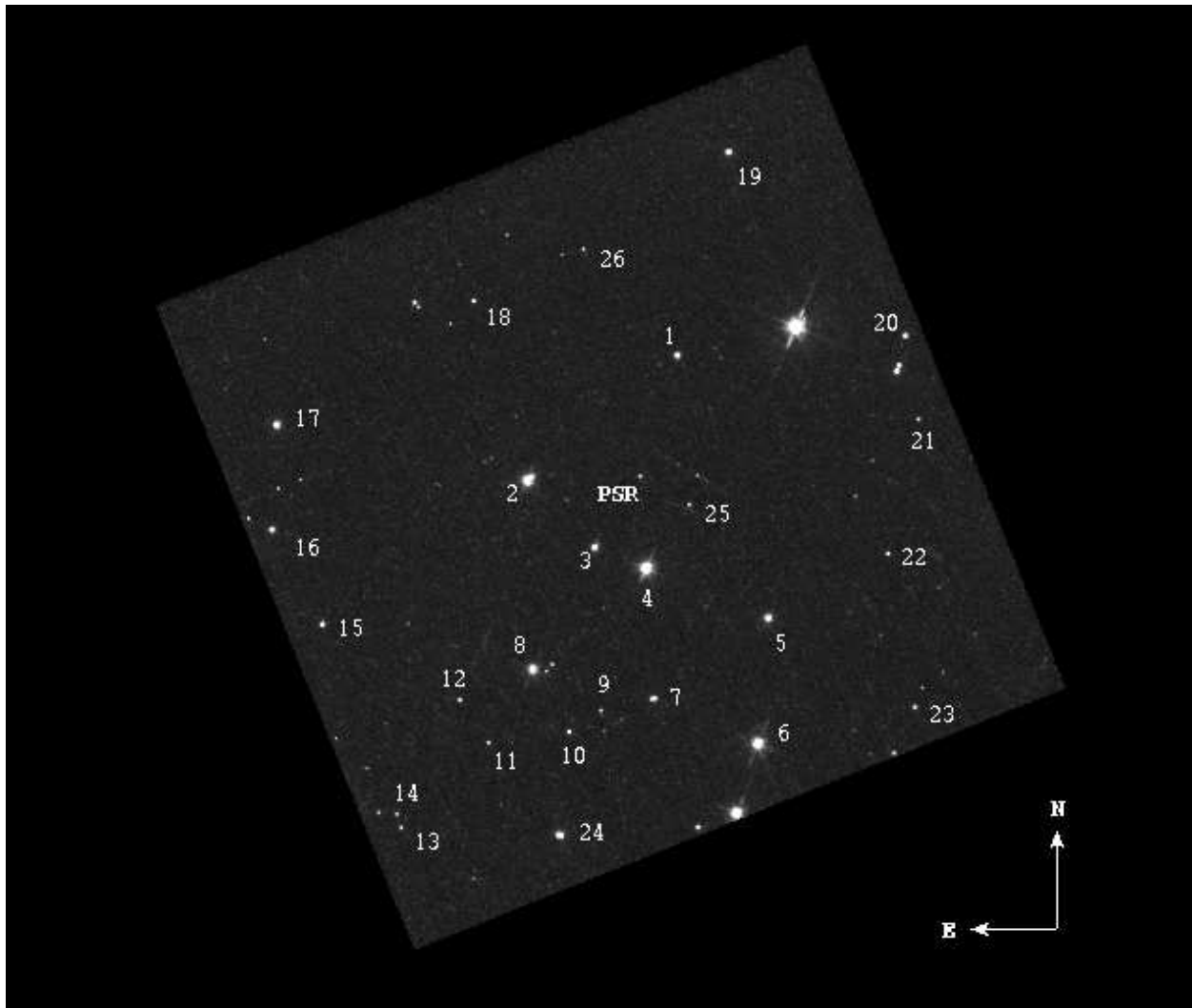


Fig. 2.— Image of the field of the Vela pulsar taken with the Planetary Camera of the WFPC2 and filter 555W. The pulsar and the reference stars used for astrometry are labelled.

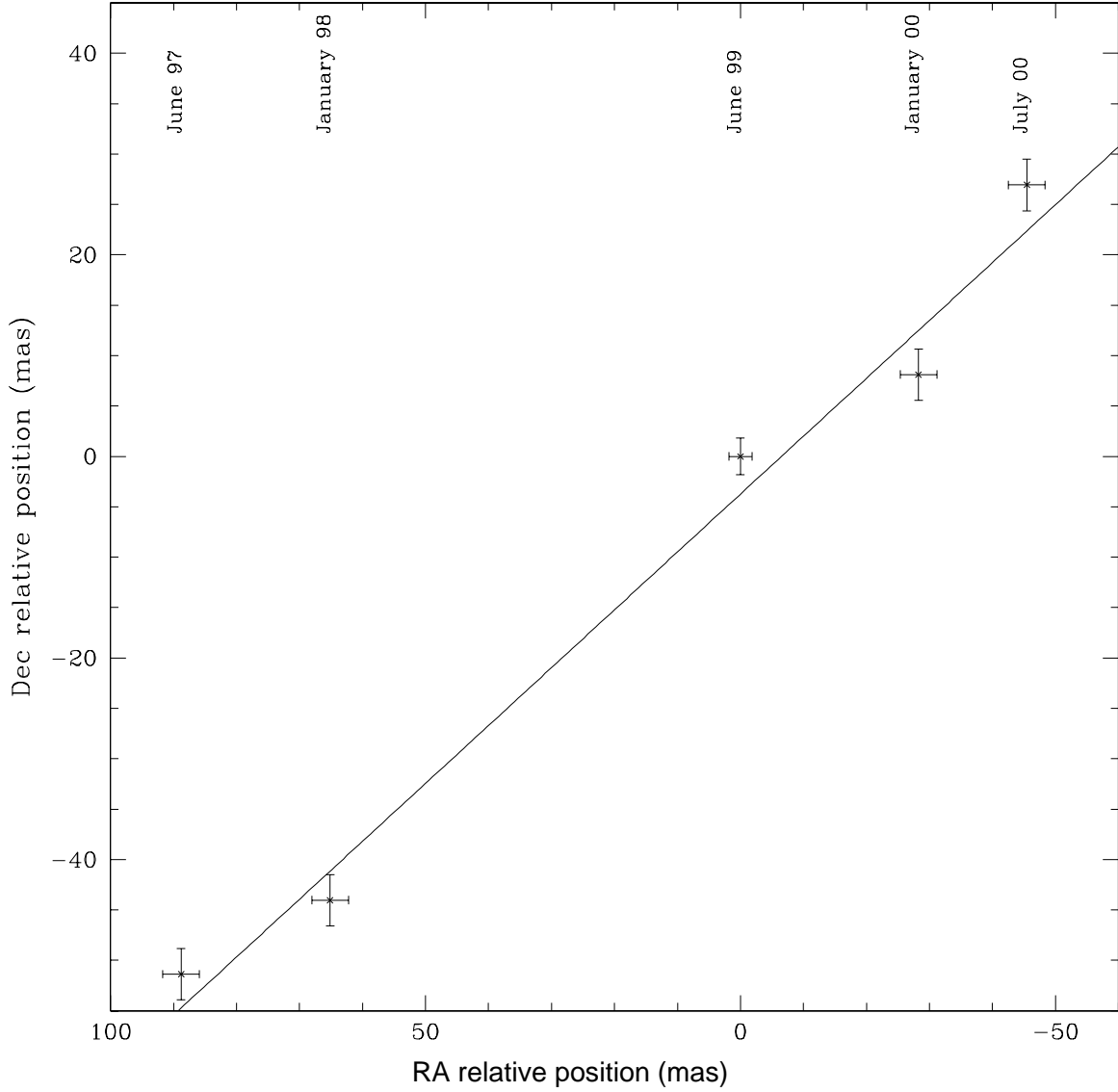


Fig. 3.— Relative positions of the pulsar obtained at the five epochs. North to the top, East to the left. The error bars account for the overall errors in the pulsar positioning. For the reference epoch (1999 June 30), the error bars (0.04 pixel, ≈ 1.8 mas) reflect only the centering uncertainties while for the other epochs (0.06 \div 0.07 pixel, $\approx 2.5 \div 2.9$ mas) we have accounted also for the errors arising from the frame registrations. The solid line corresponds to the best fit proper motion (De Luca et al. 2000b).

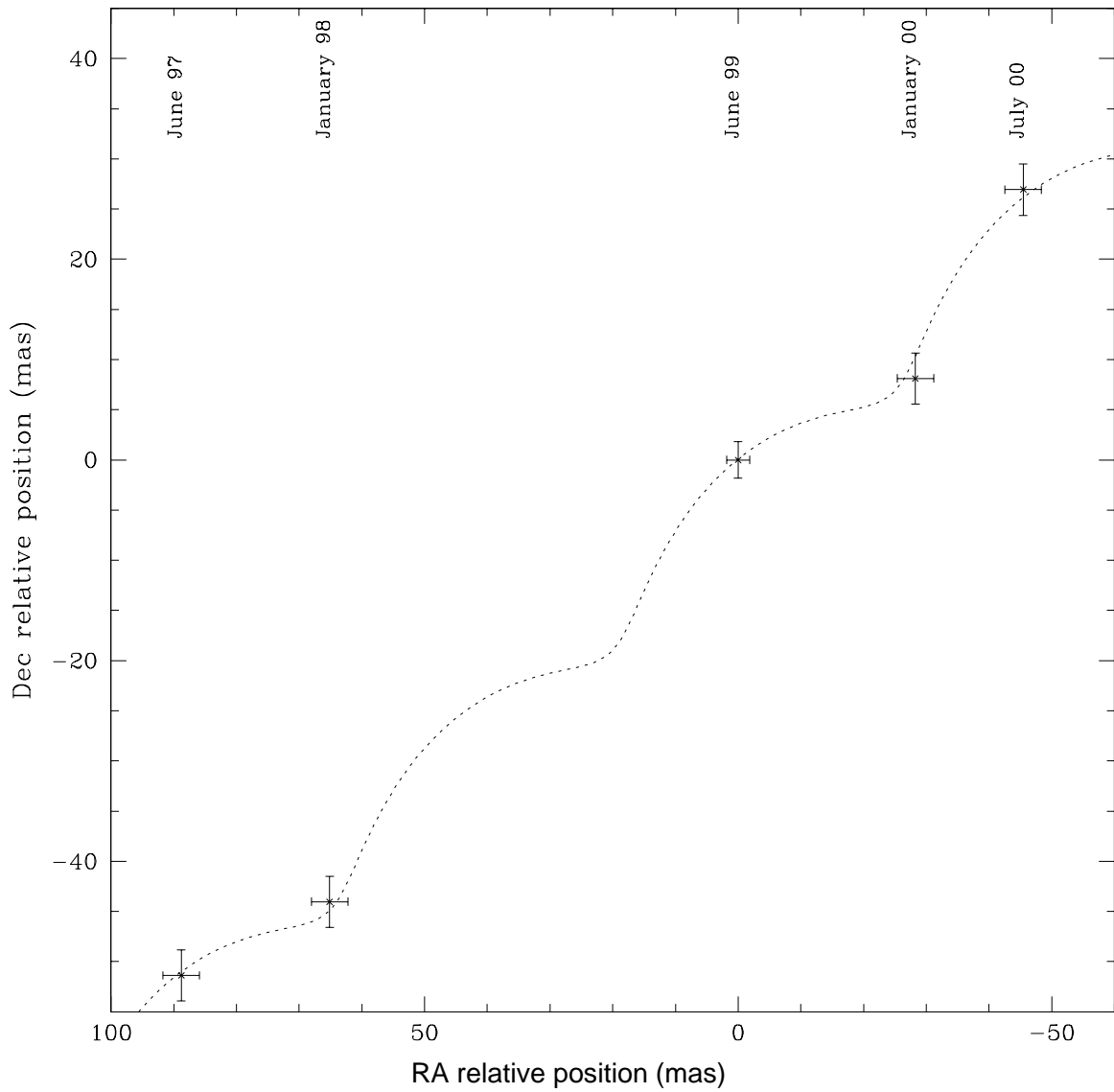


Fig. 4.— Same points as in Figure 3. The dashed line has been derived using our best fitting parallax and proper motion values.

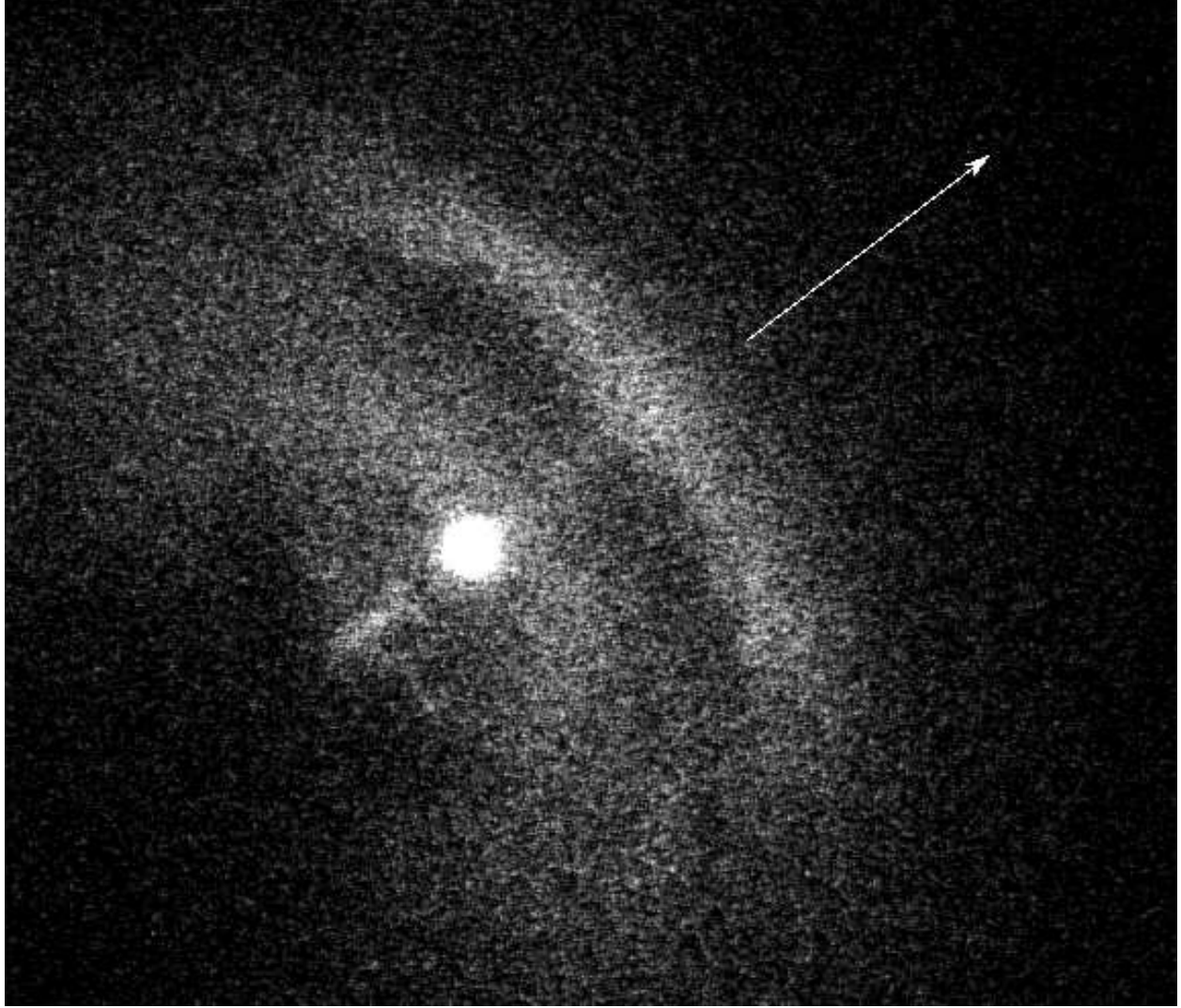


Fig. 5.— X ray image of the Vela pulsar and synchrotron nebula taken with the Chandra High Resolution Camera (North to the top, East to the left). The image has been smoothed with a low-pass filter in order to highlight the large scale structures. The arrow indicates the direction of the pulsar proper motion corrected for the peculiar motion of the Sun as discussed in Section 5.3.

Obs. ID	Date	P_α	P_δ	N.of exp.	Exposure(s)
1	1997 June 30	-0.467	0.850	2	1300
2	1998 January 2	0.399	-0.852	2	1000
3	1999 June 30	-0.478	0.852	2	1000
4	2000 January 15	0.196	-0.887	2	1300
5	2000 July 5	-0.394	0.883	2	1300

Table 1: Summary of the HST/WFPC2 observations used for the measurement of the Vela pulsar parallax. In all cases the observations were taken with the same instrument set-up, i.e., through the $F555W$ filter and with the target positioned at the center of the Planetary Camera. For each observation, the columns give the sequence number, the observing epoch and the corresponding parallactic factor in right ascension and declination (P_α, P_δ), the number of repeated exposures and exposure time in seconds. Observations #1 to #4 are the ones used by De Luca et al. (2000a) and De Luca et al. (2000b) to reassess the Vela pulsar proper motion.